Journal of
Materials Chemistry A

Accepted Manuscript

This is an *Accepted Manuscript*, which has been through the RSC Publishing peer review process and has been accepted for publication.

Accepted Manuscripts are published online shortly after acceptance, which is prior to technical editing, formatting and proof reading. This free service from RSC Publishing allows authors to make their results available to the community, in citable form, before publication of the edited article. This *Accepted Manuscript* will be replaced by the edited and formatted *Advance Article* as soon as this is available.

To cite this manuscript please use its permanent Digital Object Identifier (DOI®), which is identical for all formats of publication.

More information about *Accepted Manuscripts* can be found in the **Information for Authors**.

Please note that technical editing may introduce minor changes to the text and/or graphics contained in the manuscript submitted by the author(s) which may alter content, and that the standard **Terms & Conditions** and the **ethical guidelines** that apply to the journal are still applicable. In no event shall the RSC be held responsible for any errors or omissions in these *Accepted Manuscript* manuscripts or any consequences arising from the use of any information contained in them.

Synthesis of polyaniline nanotubes by self-assembly behavior of vitamin C: A mechanistic study and its application in electrochemical supercapacitor

Md Moniruzzaman Sk, Chee Yoon Yue*

School of Mechanical and Aerospace Engineering, Nanyang Technological University,

50 Nanyang Avenue, Singapore 639798

Abstract

Herein, we report the discovery of an unprecedented behavior of vitamin C which forms a rod-like assembly through hydrogen-bonding in water, which produced polyaniline (PANI) nanotubes upon the addition of aniline monomer by the oxidative polymerization method. It was observed that the tubular growth of PANI at the nanometer scale can be controlled by the variation of molar ratio of vitamin C to aniline. At the molar ratio of 0.25 (i.e. [Vitamin C]/[Aniline] = 0.25), long and uniform nanotubes which extends to several micrometers with an outer diameter (OD) in the range of 80 – 120 nm were observed. We have also demonstrated efficient electrochemical properties of novel PANI nanotube based electrodes which showed a higher capacitance and energy density values of 714.68 and 99.34 Wh/kg at 0.5 mA respectively. The observed results were compared and justified with the theoretical capacitance value.

*Corresponding author: Tel: +65 6790 6490 Fax: +65 67924062 E-mail address: mcyyue@ntu.edu.sg

1. Introduction

The fascinating physical and chemical properties of conducting polymers[1-3] have made possible a wide range of applications of these materials in the leading edge of electronics, optics, and energy conversion/storage[4-9]. In particular, nanostructured conducting polymers have offered unique opportunities for innovative applications in various areas, which mainly result from their beneficial characteristics at the nanometer level[10-14]. The most striking characteristic is that the properties of these materials are dependent on their size and shape (i.e. nanoparticles, nanofibers, nanotubes) when their dimensions are minimized to the nanoscale[15].

Polyaniline (PANI) is one of the most useful conducting polymers due to its high conductivity, environmental stability, and interesting redox behavior[16,17]. Nanostructured polyaniline has received much more attention over its bulk counterpart because of its many potential applications. So far different PANI morphologies have been fabricated by varying the synthesis route. Existing chemical methods of fabricating polyaniline nanostructures (particles, rods, wires, fibers, tubes) can be categorized mainly as techniques which utilize hard templates[18-24] and soft templates[25-30]. In the hard template approach, various authors have reported several types of templates including porous membranes[22] and zeolite channels[21]. Although the dimensions and morphology of polymer nanostructures can easily be tuned by the types of template, all of these approaches require some form of post-treatment of samples that are often not straightforward and may damage the soft polymeric nanostructures. Therefore, recently much attention has been paid to produce PANI nanotubes with the aid of various structure-directing soft templates such as micelles[26], vesicles[27], aniline oligomers[28,30] eliminating the use of hard template.

Xia et al.[31] reported the synthesis of an ordered whisker-like polyaniline grown on the surface of mesoporous carbon, while Gupta and Miura[32] showed an electrochemical deposition of a random nanofiber network of polyaniline. Wan et al.[29] proposed that micelles are formed from aniline monomer and organic acids in the reaction medium, and act as a template for the subsequent growth of PANI nanostructures. However, nowadays, the biomolecules based template is very promising for the synthesis of conducting polymer nanostructures due to its availability and environment friendly property.

Herein, we have developed a soft template based technique which is an easy and highly reproducible synthetic route capable of producing uniform PANI nanotubes in presence of an

easily available and low cost biological molecule, vitamin C (*l*-enantiomer of ascorbic acid). Vitamin C is an important biological antioxidant that protects the cell from detrimental radicals[33,34]. In the literature [35,36], it was reported that the vitamin C derivatives produce the self-assembled supramolecular aggregates like monolayers, micelles, vesicles, microemulsions or liposomes. For example, the octanoyl-ascorbic acid forms nearly spherical micelles in water solutions[35]. However, in our study, it was discovered that vitamin C molecules self-assemble together forming a rod-like structure through H-bonding, which can be used as a new and reliable model for the single step synthesis of polyaniline nanotubes. The detailed mechanisms for the formation of nanotubes that includes the effect of concentration of vitamin C on the overall morphology have been investigated carefully. The current work has been further extended to evaluate this novel PANI nanotube as an efficient electro-active material for the model energy-storage device, a supercapacitor[8,9]. The PANI nanotube based electrodes showed significantly improved capacitance behavior with good charge-discharge cycle life.

2. Materials and Experimental

Materials

Aniline monomer, vitamin C, ammonium persulphate (APS), nafion solution (5% in ethanol) and sulphuric acid (H_2SO_4), hydrochloric acid (HCl) were purchased from Sigma-Aldrich, Singapore. The carbon black was purchased from Age D'or Pte Ltd, Singapore. The electrochemical cell including the reference electrode, counter electrode and working electrode were purchased from Technoscience, USA.

Synthesis of PANI Nanostructures

For the synthesis of PANI nanotubes, 35 ml distilled water was treated in a beaker and stirred for 1 hour at room temperature. Then 151 µL (a constant amount for all the samples) of aniline was added and again stirred for about 30 minutes. Next, 5 ml of 0.378 g aqueous solution of APS (mole ratio of aniline : APS = 1 : 1) was added drop by drop into the reaction mixture and the resultant solution was allowed to stand for 24 hours. Then, the resulting precipitate was washed several times with distilled water to remove the core part (template) of the vitamin C/polyaniline composite. After this, 2 ml of 1 M HCl was added to the product in order to ensure complete doping (previously doped by acidic H^+ ions from vitamin C forming anilinium ions). Finally, the

pure PANI nanotube product was dried in an oven at 55°C overnight and stored. Six different molar ratios of [Vitamin C]/[Aniline] = 1, 0.5, 0.25, 0.1, 0.05 and 0.01 were used to demonstrate the effect of concentration on the polyaniline morphology. For the molar ratios of [Vitamin C]/[Aniline] = 0.5, 0.25, 0.1, 0.05 and 0.01, the corresponding samples were denoted as $PANI^{0.5}$, $PANI^{0.25,}$ $PANI^{0.1,}$ $PANI^{0.05,}$ $PANI^{0.01}$ respectively.

Characterization techniques

The field emission scanning electron microscope (FESEM) study was performed using the JEOL JSM 7600 FESEM to observe the surface morphology of the polyaniline samples. The transmission electron microscope (TEM) study was carried out using the JEOL JEM 2010 TEM to observe the bulk morphology of the polymer. The UV-Visible spectrum of the $PANI^{0.25}$ sample was obtained by dispersing about 1.0 mg sample in 10 ml distilled water using a UV-VIS-NIR scanning spectrophotometer (UV-3101PC). Fourier transform infrared spectroscopy (FTIR) study was done using the NICOLET 6700 FTIR (Thermo scientific) to investigate the chemical structure of the samples. The X-ray photoelectron spectroscopy (XPS) study was performed for the samples using the Kratos Axis-ULTRA XPS analyzer after plasma cleaning for 300 s in the XPS chamber at a pressure of about 4×10^{-8} Torr. The Brunauer-Emmett-Teller (BET) surface area, Barret-Joyer-Halenda (BJH) pore size and pore size distributions of the materials were characterized by nitrogen adsorption using a surface area and porosity analyzer (Micromeritics, ASAP 2020). The electrochemical study of the sample was investigated using the three-electrode cell by using a galvanostat/potentiostat (Gamry Reference 3000). The electrochemical performance was determined in aqueous 1 M H_2SO_4 solution using cyclic voltammetry (CV), cyclic charge-discharge (CCD) and electrochemical impedance spectroscopy (EIS) experiments. The synthesized materials were tested using the glassy carbon electrode as the working electrode, platinum as the counter electrode and a silver-silver chloride (Ag/AgCl) as the reference electrode. Thermogravimetric analysis for the samples was accomplished using the TGA 2950 over the temperature range up to 800°C at the heating rate of 10°C/min under nitrogen atmosphere.

Electrode preparation and electrochemical measurements

The electrodes were prepared with 2 mg of composite using a few drops of nafion solution (5% in ethanol) & 10 wt% carbon black to make a homogeneous paste and it was then applied on to the glassy carbon electrode (diameter 3 mm). Next, all the electrodes were dried in the oven at 90°C. A three electrode based CV experiment of the electrodes were carried out at different scan rates within the potential range of 0.0 V - 1.0 V. The similar potential range was also used for cyclic charge-discharge measurement at various discharge currents. From the discharging curve, the specific capacitances (C_{sp}) and energy density (E) were calculated[37-39] based on the relationships, $C_{sp} = (I \times t)/(V \times m)$ and $E = 1/2C_{sp}V_i^2$, where, I is the constant discharge current, t = discharging time, V = discharging voltage (excluding ohomic drop at the beginning of the discharge curve), m is the mass of the active electrode material and V_i = applied voltage. The impedance spectroscopy measurements were performed using a sinusoidal signal of 10 mV over the frequency range from 100 kHz to 1 Hz.

3. Results and discussion

Molecular characterizations

FTIR study

The molecular structure of the pure vitamin C, vitamin C/PANI composite (a product obtained before washing) and PANI nanotubes were characterized by FTIR as shown in Figure 1. The characteristic peaks (Figure 1c) at about 1583 and 1498 cm^{-1} in polyaniline nanotube were attributed to the C=C stretching for quinoid ring and the C=C stretching vibration mode for benzenoid rings indicating the presence of polyaniline[40,41]. The presence of these characteristic bands implied that the polyaniline have the amine and imine nitrogen units in its backbone. In Figure 1c, the aromatic C-H bending in the plane (1130 cm^{-1}) and out of plane (824 cm^{-1}) for a 1,4-disubstituted aromatic ring indicates a linear structure for all the polymers[41]. The characteristic peak (Figure 1c) appearing at about 1296 cm^{-1} was due to the C-N stretching of a secondary amine in the polyaniline.

The peaks that appear at 1760, 1322 and 1117 cm^{-1} in the FTIR spectra (Figure 1a) were the characteristics of C=O stretching, enol hydroxyl group and C-O-C stretching in pure vitamin C respectively[42-44]. In Figure 1a, the sharp peaks near 3500 cm^{-1} were attributed to the hydroxyl group without H-bonding, and a peak at 1634 cm^{-1} may be due to the C=C bonds in vitamin C. It should be noted that the C=C stretching in polyaniline is located at 1583 cm^{-1} (Figure 1c)

whereas in vitamin C this peak is at 1634 cm^{-1} (Figure 1a). This lowering of wave number in PANI is due to the significant delocalization of conjugated C=C bonds (in PANI). The FTIR study (Figure 1b) of vitamin C/PANI composite was also carried out in order to demonstrate the involvement of functional groups in H-hydrogen bonding, and the electron transfer mechanism (antioxidant property) of vitamin C in the reaction retardation. It is interesting to note that the C=C stretching band of pure vitamin C at 1634 cm^{-1} has disappeared in the vitamin C/PANI composite. This peak disappearance that occurred in vitamin C is probably due to the transfer of 2 electrons and 2 protons forming total 3 –C(=O)- groups[45] in the 5-membered ring (see Supporting Information, Scheme SC2). Furthermore, in the vitamin C/PANI composite the –C(=O)- peak was shifted to a lower vibrational energy (1735 cm^{-1}) (Figure 1b) compared to pure vitamin C (1760 cm^{-1}) (Figure 1a). Also, the broad peak (compared to pure vitamin C in Figure 1a) of –OH group with a shoulder at lower vibration energy (Figure 1b) was due to the polarity changes of the –OH group in the presence of H-bonding. These observations demonstrated the existence of significant intermolecular H-bonding between the –OH and –C(=O)- groups in vitamin C which resulted in the formation of a rod-like assembly.

XPS study

In order to confirm the elemental and bonding environment within the PANI nanotubes, X-ray photoelectron spectroscopy (XPS) analysis (Figure 2) was done for $PANI^{0.25}$ samples. The XPS spectrum of $PANI^{0.25}$ showed the presence of C, O and N elements (see Supporting Information, Figure S3). An N 1s narrow scan core-level spectrum (Figure 2) showed that most of the nitrogen atoms were in the form of amine (-NH-) centered at 400.04 eV in benzenoid amine or amide groups[15,46]. Two small additional peaks[15,46] (Figure 2) suggested that some nitrogen atoms existed as imine (=N-) form centered at 399.3 eV and positively charged nitrogen (N^+) form centered at 401.08 eV.

Spectral characterizations

UV-visible study

The UV-visible spectrum of PANI nanotubes ($PANI^{0.25}$) was recorded (Figure 3) by dispersing it in an aqueous medium which demonstrated two main characteristic absorption peaks at about 312 nm and 452 nm. One was due to π–π transition at 312 nm in the benzenoid rings and the

other was assigned as polaron band (polaron–π* transition)[47,27,15] at 452 nm. A broader peak at higher wavelength near 800 nm corresponded to the π-polaron transition of the quinoid ring. It demonstrated that the polyaniline chains were in the doped state. The polaronic transitions (polaron-π* and π-polaron) clearly indicates the presence of charge carriers in the polymer, the π-π* transition arose from neutral benzenoid segments[47,27,15]. Furthermore, the ratios of the absorbance of the polaronic band to that of the π-π* band were estimated which provided a measure of the average oxidation level of the polyaniline nanostructure. It is apparent from Figure 3 that the absorbance peak intensity ratios of $A_{452\ nm}/A_{312\ nm}$ and $A_{800\ nm}/A_{312\ nm}$ were found to be > 1, which revealed that the polyaniline nanotubes appeared to be in the higher oxidation level.

Morphological investigation and mechanism

To synthesize the PANI nanotubes, six different molar ratios of [Vitamin C]/[Aniline] were used with a fixed molar ratio of [Aniline]/[APS] = 1:1 and the same reaction temperature (room temperature). Nanotubes with different morphologies were obtained. It was found that the size and uniformity of polyaniline nanotubes could be appropriately adjusted by tuning the concentration of aniline and vitamin C. Except at a molar ratio of [Vitamin C]/[Aniline] = 1 (where no polymerization occurred), all the other ratios produced polyaniline with different morphologies depending on the ratio used. The length of the nanotube was significantly influenced by the [Vitamin C]/[Aniline] ratio and the average length varied from a few nanometers to several micrometers when the molar ratio was varied from 0.5 to 0.01. The longer (several micrometers) and uniform nanotubes (OD: 80-120 nm) (as can be seen in Figure 4 and Figure 5) were found at the molar ratio of [Vitamin C]/[Aniline] = 0.25. It is noteworthy that, in addition to this, uniform nanotubes were also produced at the molar ratio 0.1. However, the length of the nanotubes for the ratio 0.25 was longer than that obtained at 0.1. These results indicated that a molar ratio in the range of 0.1 – 0.25 was favorable for the formation of PANI nanotubes, and the optimum was obtained at a 0.25 ratio.

Shorter length nanotubes or random aggregates of thick polymer layer were formed at the ratios of 0.5, 0.05 and 0.01 (Figure 4 & Figure 5). This may be due to presence of either very high or very low concentrations of vitamin C in the reaction medium whereupon proper association of vitamin C molecules cannot take place in both cases. At higher concentration (see

Figure 4a) it appeared that many rod-like vitamin C assemblies fused together, which destroyed the orientation of individual assembly. And at lower concentration (see Figure 4e), the deficiency of vitamin C seems to have created an improper assembly that resulted in the formation of random aggregates of polyaniline.

It was observed that no reaction occurred at a molar ratio of 1. The presence of equal amounts of oxidant and antioxidant ([APS]/[Vitamin C] =1 i.e. [oxidant]/[antioxidant] = 1) in the reaction medium probably caused the rate of oxidation reaction of APS and the reduction reaction of vitamin C to be the same at this molar ratio such that it cancelled out the net oxidation of aniline monomer for further polymerization (see Supporting Information, Scheme SC1). A delay in response in the polymerization reactions (recognized by color change that occurred in the reaction medium) was observed at each different molar ratio after the addition of initiator (APS). This may be due to the antioxidant properties of vitamin C which partially reduced the anilinium radical ions that were previously produced due to the presence of APS. Each synthesis (with each different molar ratio) was repeated 6 times and the delay in reaction times were recorded (Figure 6). It can be seen from Figure 6 that, at lower molar ratio, the delay time of the reaction after addition of APS was negligible, whereas at higher concentration, this was longer.

The probable mechanism for the formation of nanotube can be postulated from the observed development of the aggregation of vitamin C molecules into solid rod-like assemblies (Scheme 1) through intermolecular H–bonding among several –OH/-(C=O)- groups. After the addition of aniline monomer, it (monomer) interacts on the outer surface of the rod-shaped vitamin C to form an aniline wrapped vitamin C composite assembly. Due to the shape-persistent features and fixed orientation of non-covalent interaction sites in aniline molecule, it was self-assembled into the tubular structures, which was governed by H-bonding between the oxygen of –OH, =O groups in vitamin C and the protonated anilinium ions (and aniline molecules if present). The enolic –OH group (see Supporting Information, Scheme SC2) is more acidic (due to keto-enol tautomerization) than the typical –OH groups and upon the addition of aniline monomer in the solution of vitamin C, it abstracted H^+ ions to form anilinium ions. The aniline monomer also abstracted one more proton (per molecule) from vitamin C (see Supporting Information, Scheme SC2). This anilinium ion could then initiate the polymerization reaction in the presence of APS.

The H-bonding mechanism was verified using the following approaches utilizing a fixed molar ratio of [Vitamin C]/[Aniline] = 0.25:

A) *Effect of solvent polarity:* The polymerization was carried out in different solvents like ethanol, 2-propanol and acetone at the molar ratio of [Vitamin C]/[Aniline] = 0.25 under the same condition as water medium. The FESEM micrographs (see Supporting Information, Figure S1) of each product (final product after washing) were taken and it was observed that no nanotubes were found which supported the important role of the H-bonding mechanism. This may be explained as the H-bond formation tendency is higher in a more polar solvent than in a less-polar/non-polar solvent. Herein, the polarity and H-bond formation tendency of the different solvents used are increased in the order of acetone < 2-propanol < ethanol < water. At the initial stage, the more polar solvent (water) formed intermolecular H-bonding with the vitamin C, which changed the polarity of the –OH or –C(=O)- groups (in vitamin C). This change of polarity consequently facilitated the association of vitamin C through intermolecular H-bonding (among vitamin C) which was not the case in other solvents. Thus, only water solvent produced the polyaniline nanotubes.

B) *Effect of dilution:* At higher dilution with increased solvent (water) amount from 40 ml to 250ml in vitamin C & aniline mixture, no formation of nanotube was observed (see Supporting Information, Figure S2) and instead, the formation of random aggregates of polyaniline was found. This may be due to the low concentration of vitamin C in water which caused high dilution and disallowed the efficient formation of H-bonding.

C) *Nature of intermediate products:* Furthermore, a careful investigation of the reaction mechanism was carried out at different stages of the reaction at the selected molar ratio of [Vitamin C]/[Aniline] = 0.25 in water in order to derive some insightful understanding of the reaction mechanism. After the addition of initiator (APS), the reaction products at various reaction times (t =10 minutes, t = 1 hour, t = 4 hours and t = 24 hours) were collected, washed and dried after which they were examined under the TEM (see Figure 7). At t = 10 minutes, a very narrow vitamin C-PANI nanofibers is formed and continuous assemble of aniline onto the vitamin C is occurring, at t = 1 hour the vitamin C-PANI nanofibers formation is finished and this is also same as at t = 4 hours. At t = 24 hours, after washing the core part vitamin C (water soluble), the PANI nanotubes were formed. This continuous monitoring of the reaction as the

reaction progressed strongly supported the association of vitamin C through the intermolecular H-bonding.

Electrochemical characterizations

Cyclic voltammetry (CV) experiment

The current-voltage response of $PANI^{0.25}$ electrode was examined by CV experiment using a three-electrode electrochemical cell within the potential range of 0 – 1.0 V in an aqueous 1 M H_2SO_4 electrolyte. The CV curves of PANI nanotubes at the scan rates of 5, 10, 20, 50, 100 and 200 mV/s are shown in Figure 8a. The lack of symmetry (i.e. deviation from rectangularity) in the CV curves (Figure 8a) was largely due to the pseudo-capacitive property of polyaniline. No obvious peaks were observed at higher scan rates, which may be attributed to the fast electrochemical process which is not able to display the detailed electrochemical phenomena[48]. On the other hand, at lower scan rate (≤ 50 mV/s) some peaks appeared due to the slow process where perhaps an active participation of electrolyte and electrode occurred during the test.

It is noticeable from Figure 8a that the peak intensity was gradually increasing as we moved towards the lower scan rate. The appearance of a peak at lower scan rate for $PANI^{0.25}$ electrode was probably due to the electronic transition between different oxidation states of PANI chains. A pair of broad redox peaks (each pair consisting of an anodic and a cathodic peak) was found for the sample at the lower scan rate (Figure 8a). In general, polyaniline shows two redox processes[15,49], namely; (i) leucoemeraldine (LE)/emeraldine salt (ES) transition and (ii) emeraldine salt (ES) /pernigraniline (P) transition. Herein, the observed broad redox peaks (obvious in Figure 8a at 20 mV/s) originated from the overlap of the two redox processes[15]. Therefore, in order to derive more details on electrochemical mechanisms, a lower scan rate is always more preferable.

For the $PANI^{0.25}$ based electrode, the CV profiles proved to show good electrochemical behavior which was apparent from Figure 8a which exhibited high current values of 0.012 A @ 200mV/s & 0.0016 A @ 5 mV/s. Furthermore, as seen in Figure 8b, both the anodic and cathodic peak currents increased near linearly with scan rate, implying good reversible stability and fast response to oxidation/reduction on the current changes due to surface-controlled redox process[15,50.] The redox process has been found to take place at the surface of the electrode, which was most likely due to the low dimension of the polyaniline nanotubes.

Cyclic charge-discharge study (CCD)

The galvanostatic charge/discharge experiments (Figure 9) for the $PANI^{0.25}$ electrode were conducted in an aqueous 1 M H_2SO_4 electrolyte. The experiments were accomplished with three different charge-discharge currents of 1 mA, 0.75 mA and 0.5 mA. The nanotube electrode was found to have a specific capacitance of 619.76 F/g at 1 mA constant charge-discharge current. The specific capacitance was found to increase with decreasing current. When the current was decreased from 1 to 0.5 mA, the specific capacitance showed an increase in capacitance from 619.76 F/g to 714.68 F/g respectively. The capacitance was 643.18 F/g when the current was 0.75 mA. An excellent energy density of 99.34 Wh/kg was obtained for $PANI^{0.25}$ electrode at a discharge current of 0.5 mA. Also, at the discharge current of 0.75 mA and 1 mA, the energy density values were 89.4 Wh/kg and 86.14 Wh/kg respectively.

Furthermore, although all the curves showed the ohomic drops (due to the internal resistance) at the beginning of the discharging phase, however this was reduced at the lower charge-discharge current of 0.5 mA. This increase in specific capacitance and lowering of ohomic drop at lower current value may be attributed to the slow electrochemical process in which the electrolyte ions accessed the deep pores (in the inner surface of the nanotubes) of the electrode. It is important to note that the ions had accessibility of the entire electrode surface area (both the outer surface and inner surface). On the other hand, at higher charge-discharge current (fast electrochemical process), the electrolyte ions only have time to access the outer surface area of the electrode which leads to a lower capacitance value[51,48.] Furthermore, as discussed in a following section, the maximum theoretical value for the nanotube electrode can be calculated and correlated with the observed experimental value.

Justification between theoretical and observed capacitance value

The significantly high specific capacitance value of 714.68 F/g reported above can be justified through theoretical considerations. The maximum theoretical capacitance can be calculated by considering Faradaic reactions or pseudo-capacitance (C_{pseu}) in parallel to the double layer capacitance (EDLC) for a porous conducting polymer electrode, leading to an upper limit of the capacitance value. Although the actual combination of the two elements (C_{pseu} & EDLC) could be more complicated, the maximum theoretical specific capacitance (C_{max}) can be estimated using the following formula[52,53]:

$C_{max} = \alpha.F/dV.M + C_{dl}.A$ ---------- (1)

where α is the fraction of electron shared on each monomer unit, F is the Faraday constant (96485.3 C/mol), dV is the voltage range, M is the molecular weight of aniline repeat units (91.1 g/mol), A is the specific surface area and C_{dl} is the double layer capacitance. The maximum value of α is 1 in PANI. The average C_{dl} of PANI was reported to be about 30 μF/cm^2. The average specific surface area for the PANI$^{0.25}$ was found to be 39.75 m^2/g by BET measurement (which was about 3-fold higher than the pristine PANI synthesized without template) (see Supporting Information, Figure S4). Therefore, the theoretical C_{max} was estimated to be 1071.039 F/g within the potential of 1 V, wherein the pseudocapacitance contribution was 1059.114 F/g and the double layer capacitance was only 11.925 F/g.

According to the well-studied redox mechanism of polyaniline, 1 electron per monomer (i.e. α = 1) is needed to oxidize the polymer from its fully reduced leucoemeraldine state (LE) to its fully oxidized pernigraniline (P) state. The value of α is known to be related to the insulating-to-conducting phase transition in the polymer. When α =1, this phase transition is low in electrochemical reversibility[54]. This α value varies through the conversion from LE to emeraldine state (ES) with $0 < \alpha < 0.5$ and ES to P with $0.5 < \alpha < 1$. The more reversible conversion between LE and ES involves 0.5 electron per monomer[54] (i.e. α = 0.5).

However, in our experiment, the specific capacitances were found to be 619.76 F/g at 1 mA, 643.18 F/g at 0.75 mA and 714.68 F/g at 0.5 mA which are all lower than the maximum possible value of 1071.039 F/g. Based on the observed capacitance values and using equation (1), the degree of oxidations per monomer α at the different discharge currents were calculated and the results are as shown in Table 1. It is apparent from Table 1 that at 1 mA discharge current, 57.39% electron transfer occurred per monomer (i.e. α = 0.5739) in polyaniline. This implies that only 57.39% of electrons was active for the redox capacitance. At 0.5 mA, the proportion of active electrons increased to 66.35% (i.e. α = 0.6835). This demonstrated that at a lower discharge current and higher oxidation level, the capacitance value is increased.

The lower observed value of 714.68 F/g (at 0.5 mA) compared to the theoretical value of 1071.039 F/g can be accounted for by the lower experimentally observed of α value (i.e. $\alpha < 1$). The theoretical capacitance in our experiment can probably be achieved at some very low discharge current when α =1 (i.e. when all the PANI chains are accessible and are in a highly doped state). Although the high pseudocapacitance value of the polyaniline nanotube could push

the total capacitance to the theoretical value at an extremely low current density (where $\alpha \approx 1$), however, such a low current defeats the primary purpose of using a supercapacitor for high charge/discharge rate applications.

Furthermore, the lower observed capacitance value could be explained by the ion transport phenomenon within the nanotube electrode. Typically, the polyaniline nanotubes are randomly oriented (as may be the case in our study) with respect to the current collectors in a supercapacitors electrode[55,56]. In such cases, the electrolyte ions are often limited from penetrating far inside the polyaniline chains. This lowers the complete utilization of the electrode surface area. It has been reported that ion diffusion parallel to the orientation of nanotube can be exceedingly fast which consequently produces large capacitance value[55,56].

Impedance spectroscopy (EIS)

To demonstrate the impedance characteristics[57-59] of mesoporous $PANI^{0.25}$ electrode, electrochemical impedance measurements (EIS) were carried out in 1 M aqueous H_2SO_4 electrolyte. Herein, two Nyquist plots (see Figure 10) are shown, the first plot was carried out at the 1st cycle and second plot after the 500th charge-discharge cycle. Both the curves in Figure 10 displayed almost similar low frequency impedance characteristics but a different profile in the high frequency region. The Nyquist plots (Figure 10) contain two segments, namely: a lower frequency region on the upper right portion, and a high frequency region on the lower left portion of the plot. Both the graphs exhibited a semi-circle at the high frequency range followed by a linear slope in the low frequency region. The resistance characterized by the semi-circle is commonly known as charge transfer resistance (Rct). A small semi-circle for the electrode at the 1st cycle suggested very low (Rct = 0.78 ohm) interfacial charge-transfer resistance due to the good electrode/electrolyte contact. However, after the 500th cycle, the appearance of a slightly larger semicircle (Rct = 1.29) may be caused by the onset of a little swelling/shrinkage in the electrode material under continuous charge-discharge cycles.

The intercept at Zreal along the X-axis at very high frequencies is known as the equivalent series resistance (ESR). This resistance originates from a combination of: (a) ionic resistance of the electrolyte within the electrode, (b) intrinsic resistance of the material, and (c) contact resistance at the active material/current collector interface[52]. The lower ESR (15.29 ohm) found at the 1st cycle was probably due to the large surface area of the nanostructured electrode.

However, after the 500th cycle, the ESR in the cell increased slightly to 17.07 ohm. The increase in resistance can probably be attributed to partial sealing of the pores between the chains (due to the swelling/contraction of polyaniline chains) under cycling. The part of the curve with 45^{o} slope (at low frequency zone) called the Warburg resistance (W), is a consequence of the frequency dependence of the ion diffusion/transport process. The resistance to ionic diffusion is proportional to the slope of the impedance curves in the low frequency region. A more vertical line indicates that the electrode is closer to an ideal capacitor and a large deviation from the vertical line indicates a higher Warburg resistance. The slope of the plots in Figure 10 decreased slightly after 500th cycles, thereby indicating only a small increase in ionic diffusion resistance after 500th cycles. This demonstrated the excellent supercapacitive performance of the electrode even after 500 charge-discharge cycles. Thus, the nanotubular morphology of polyaniline is very promising for improved electrochemical performance.

Cyclic stability

The cycle life efficiency of the PANI$^{0.25}$ electrode was tested by 500 continuous charge–discharge cycles at a constant charge-discharge current of 1 mA. The retention of capacitance over a number of charge-discharge cycles is a crucial parameter for long term power-delivery supercapacitors. Herein, the PANI$^{0.25}$ electrode showed capacitance retention of 84.88 % (see Figure 11) after 500 continuous charge-discharge cycles. The drop in capacitance after 500 cycles may be explained by the loss of adhesion of some active material in the current collector or volumetric change (due to swelling and contraction) which caused partial blockage of the regular pore structure[60]. This caused the slow ionic transfer rate at higher cycles which eventually led to the slight reduction in capacitance.

Conclusion

We have successfully demonstrated a straight forward novel strategy to produce long uniform polyaniline nanotubes using the chemical oxidative polymerization method through the use of a biomolecule, vitamin C. The nanotubes were several micrometers long and had an outer diameter in the range of 80 - 120 nm. It was observed that the morphology of the polyaniline changed when the molar ratio of vitamin C was varied. A delay in the onset of reaction was observed at higher molar ratios of vitamin C. No reaction occurred at an equal molar ratio of vitamin C to

aniline due to the antioxidant property of vitamin C. The intermolecular H-bonding amongst the vitamin C molecules was responsible for the rod-like assembly leading to the formation of polyaniline nanotubes. The $PANI^{0.25}$ electrode showed excellent capacitive behavior (714.68 F/g at 0.5 mA) with good cycling stability. Such a PANI nanotube based electrode with good electrochemical behavior has excellent potential for various applications in nanoelectronics including supercapacitors. Moreover, we believe that this could be a model synthesis route for the large scale production of all kind of polar conducting polymers in a very simple, low cost and eco-friendly way.

Supporting Information Available: 1. FESEM micrographs to study the reaction mechanism through the effect of solvent (Figure S1), 2. FESEM micrographs to study the reaction mechanism through the effect of dilution (Figure S2), 3. XPS spectra (Figure S3), 4. Surface area measurements and pore size distributions (Figure S4), 5. Thermogravimetric analysis (Figure S5), 6. Reaction kinetics in presence of vitamin C and APS in aniline polymerization (Scheme SC1), and 7. Electron transfer mechanism (anti-oxidant property) in vitamin C (Scheme SC2).

References

1. Y. F. Li, *Prog. Chem.,* 2002, **14**, 207.

2. J. Jang, *Adv. Polym. Sci.,* 2006, **199**, 189.

3. D. E. Stilwell and S-M. Park, *J. Electrochem. Soc.,* 1988, **135**, 2491.

4. D. Aradilla, F. Estrany and C. Aleman, *J. Phys. Chem. C,* 2011, **115**, 8430.

5. M. Gerard, A. Chaubey, and B. D. Malhotra, *Biosens. Bioelectron.* 2002, 17, 345.

6. D. Y. Liu and J. R. Reynolds, *ACS Appl. Mater. Interfaces,* 2010, 2, 3586.

7. M. Mastragostino, C. Arbizzani and F. Soavi, *Solid State Ionics,* 2002, **148**, 493.

8. M. N. Hyder, S. W. Lee, F. C. Cebeci, D. J. Schmidt, Y. Shao- Horn and P. T. Hammond, *ACS Nano,* 2011, **5**, 8552.

9. H. Guan, L. Z. Fan, H. C. Zhang and X. H. Qu, *Electrochim. Acta,* 2010, **56**, 964.

10. H. Yoon and J. Jang, *Adv. Funct. Mater.,* 2009, **19**, 1567.

11. A. Mulchandani and N. V. Myung, *Curr. Opin. Biotechnol.,* 2011, **22**, 502.

12. L. Al-Mashat, K. Shin, K. Kalantar-Zadeh, J. D. Plessis, S.H. Han, R.W. Kojima, R. B. Kaner, D. Li, X. L. Gou, S. J. Ippolito and W. Wlodarski, *J. Phys. Chem. C,* 2010, **114**, 16168.

13. H. Yoon, S. H. Lee, O. S. Kwon, H. S. Song, E. H. Oh, T. H. Park and J. Jang, *Angew. Chem., Int. Ed.,* 2009, 48, 2755.

14. J. J. Xu, K. Wang, S. Z. Zu, B. H. Han and Z. X. Wei, *ACS Nano,* 2010, **4**, 5019.

15. H-W. Park, T. Kim, J. Huh, M. Kang, J. E. Lee and H. Yoon, *ACS nano,* 2012, **6**, 7624.

16. D. W. Wang, F. Li, J. P. Zhao, W. C. Ren, Z. G. Chen, J. Tan, Z. S. Wu, I. Gentle, G. Q. Lu and H. M. Cheng, *ACS Nano,* 2009, **3**, 1745.

17. D. Li, J. X. Huang and R. B. Kaner, *Acc. Chem. Res.,* 2009, **42**, 135.

18. C. R. Martin, *Science,* 1994, **266**, 1961.

19. C. R. Martin, *Acc. Chem. Res.,* 1995, **28**, 61.

20. M. Granstrom and O. Inganos, *Polymer,* 1995, **36**, 2867.

21. V. M. Cepak, C. R. Martin, *Chem. Mater.,* 1999, **11**, 1363.

22. X. Li, S. Tian, Y. Ping, D. H. Kim and W. Knoll, *Langmuir,* 2005, **21**, 9393.

23. P. Anilkumar and M. Jayakannan, *Macromolecules,* 2008, **41**, 7706.

24. X. Zhang and S. K. Manohar, *Chem. Commun.,* 2004, **20**, 2360.

25. J. X. Huang, S. Virji, B. H. Weiller and R. B. Kaner, *J. Am. Chem. Soc.,* 2003, **125**, 314.

26. H. J. Ding, J. Y. Shen, M. X. Wan and Z. J. Chen, *Macromol. Chem. Phys.,* 2008, **209**,864.

27. U. Rana, K. Chakrabarti and S. Malik, *J. Mater. Chem.,* 2012, **22**, 15665.

28. Z. D. Zujovic, C. Laslau, G. A. Bowmaker, P. A. Killmartin, A. L. Webber, S. P. Brown and J. Travas-Sejdic, *Macromolecules,* 2010, **43**, 662.

29. M. X. Wan, *Adv. Mater.,* 2008, **20**, 2926.

30. Y. F. Huang and C. W. Lin, *Polymer,* 2009, **50**, 775.

31. Y. -G. Wang, H. -Q. Li and Y. -Y. Xia, *Adv. Mater.*, 2006, **18**, 2619.

32. V. Gupta and N. Miura, *Mater. Lett.,* 2006, **60**, 1466.

33. S. J. Padayatty, A. Katz, Y. Wang, P. Eck, O. Kwon, J. -H. Lee, S. Chen, C. Corpe, A. Dutta, S. K. Dutta and M. Levine, *J. Am. Coll. Nutr.,* 2003, **22**, 18.

34. M. J. Ortner, *Exp. Cell Res.,* 1980, **129**, 485.

35. P. L. Nostro, G. Capuzzi, A. Romani and N. Mulinacci, *Langmuir,* 2000, 16, 1744.

36. K. Moribe, W. Limwikrant, K. Higashi and K. Yamamoto, *J. Drug Deliv.*, volume 2011, Article ID 138929, 9 pages, doi:10.1155/2011/138929.

37. Q. Wu, Y. Xu, Z. Yao, A. Liu and G. Shi, *ACS Nano*, 2010, **4**, 1963.

38. V. Gupta and N. Miura, *Electrochim. Acta.,* 2006, **52**, 1721.

39. T. C. Girija and M. V. Sangaranarayanan, *J. Power Sources.* 2006, **156**, 705.

40. V. S. Jamadade, D. S. Dhawale and C. D. Lokhande, *Synth. Met.,* 2010, **160**, 955.

41. S. Sathiyanarayanan, S. Muthkrishnan and G. Venkatachari, *Electrochimica. Acta.,* 2006, **51**, 6313.

42. J. Xiong, Y. Wang, Q. Xue and X. Wu, *Green Chem.,* 2011, 13, 900.

43. C. Garnero and M. Longhi, *J. Pharmaceut. Biomed. Anal.,* 2007, 45, 536.

44. B. Zumreoglu-Karan, *Coord. Chem. Rev.,* 2006, **250**, 2295.

45. A. Karlsen, R. Blomhoff and T. E. Gundersen, *J. Chromatogr. B,* 2005, **824**, 132.

46. K. Zhang, L. L. Zhang, X. S. Zhao and J. Wu, *Chem. Mater.,* 2010, **22**, 1392.

47. T. Abdiryim, Z. Xiao-Gang and R. Jamal, *Mater. Chem. Phys,.* 2005, **90**, 367.

48. X. Xiang, E. Liu, Z. Huang, H. Shen, Y. Tian, C. Xiao, J. Yang and Z. Mao, *J. Solid State Electrochem.,* 2011, **15**, 2667.

49. S. Xiong, Fan. Yang, H. Jiang, J. Ma and X. Lu, *Electrochim. Acta,* 2012, **85**, 235.

50. Y. Li, X. Zhao, Q. Xu, Q. Zhang and D. Chen, *Langmuir,* 2011, **27**, 6458.

51. Q. Li, J. Liu, J. Zou, A. Chunder, Y. Chen and L. Zhai, *J. Power Sources,* 2011, **196**, 565.

52. F. Huang and De. Chen, *Energy Environ. Sci.,* 2012, **5**, 5833.

53. C. Peng, X. Zhou, G. Z. Chen, F. Moggia, F. Fages, H. Brisset and J. Roncali, *Chem. Commun.,* 2008, **48**, 6606.

54. C. Peng, D. Hu and G. Z. Chen, *Chem. Commun.,* 2011, **47**, 4105.

55. Z. –L. Wang, R. Guo, G. –R. Li, H. –L. Lu, Z. –Q. Liu, F. –M. Xiao, M. Zhang and Y. –X. Tong, *J. Mater. Chem.,* 2012, **22**, 2401.

56. B. J. Hinds, N. Chopra, T. Rantell, R. Andrews, V. Gavalas and L. G. Bachas, *Science,* 2004, **303**, 62.

57. W. Sugimoto, H. Iwata, K. Yokoshima, Y. Murakami and Y. Takasu, *J. Phys. Chem. B.,* 2005, **109**, 7330.

58. X. Xiang, E. Liu, Z. Huang, H. Shen, Y. Tian, C. Xiao, J. Yang and Z. Mao, *J. Solid State Electrochem.,* 2011, **15**, 2667.

59. X. Xie and L. Gao, *Carbon,* 2007, **45**, 2365.

60. I. Kovalenko, D. G. Bucknall and G. Yushin, *Adv. Funct. Mater.,* 2010, **20**, 3979.

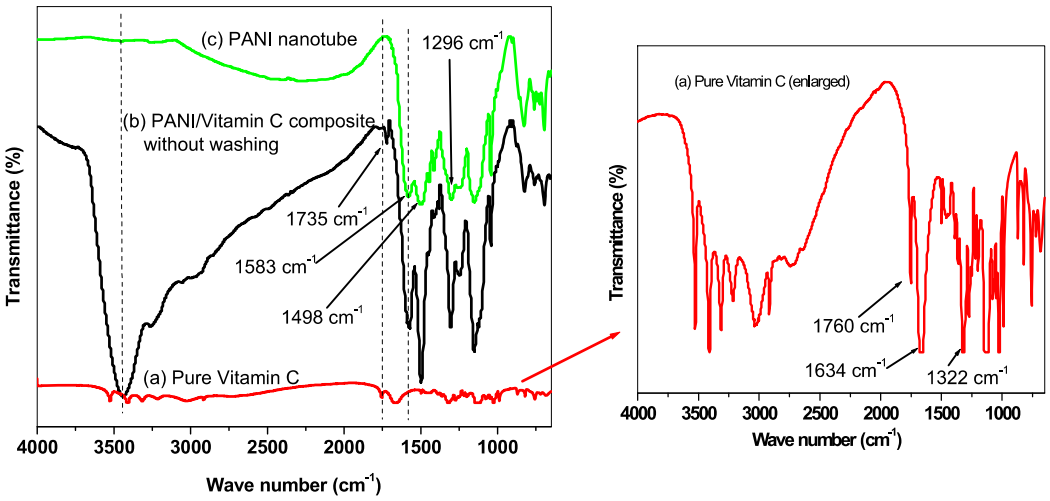

Fig. 1 FTIR spectra of (a) pure vitamin C, (b) PANI/vitamin C at the molar ratio of 0.25 without washing and (c) pure PANI nanotube ($PANI^{0.25}$) at the molar ratio of 0.25 after washing. On right side is the enlarged spectrum of pure vitamin C.

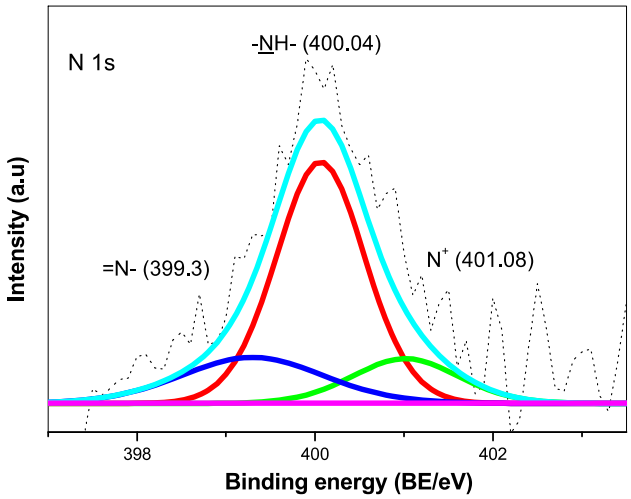

Fig. 2 XPS spectra of N 1s of $PANI^{0.25}$ (narrow scan).

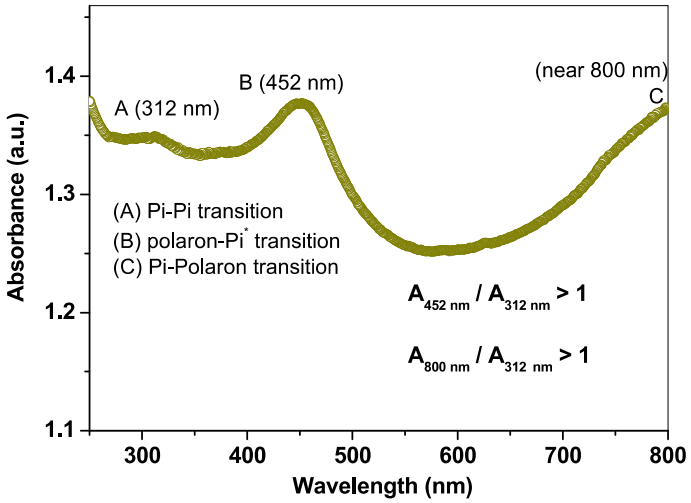

Fig. 3 UV-Vis spectra of $PANI^{0.25}$ dispersed in water solvent.

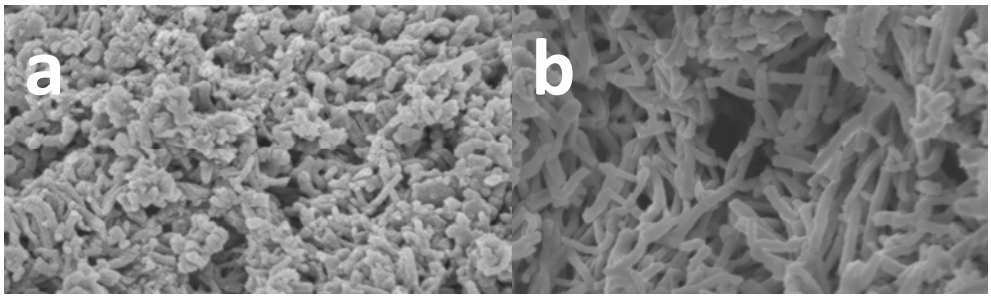

Fig. 4 FESEM images of (a) $PANI^{0.5}$, (b) $PANI^{0.25}$, (c) $PANI^{0.1}$, (d) $PANI^{0.05}$ and (e) $PANI^{0.01}$.

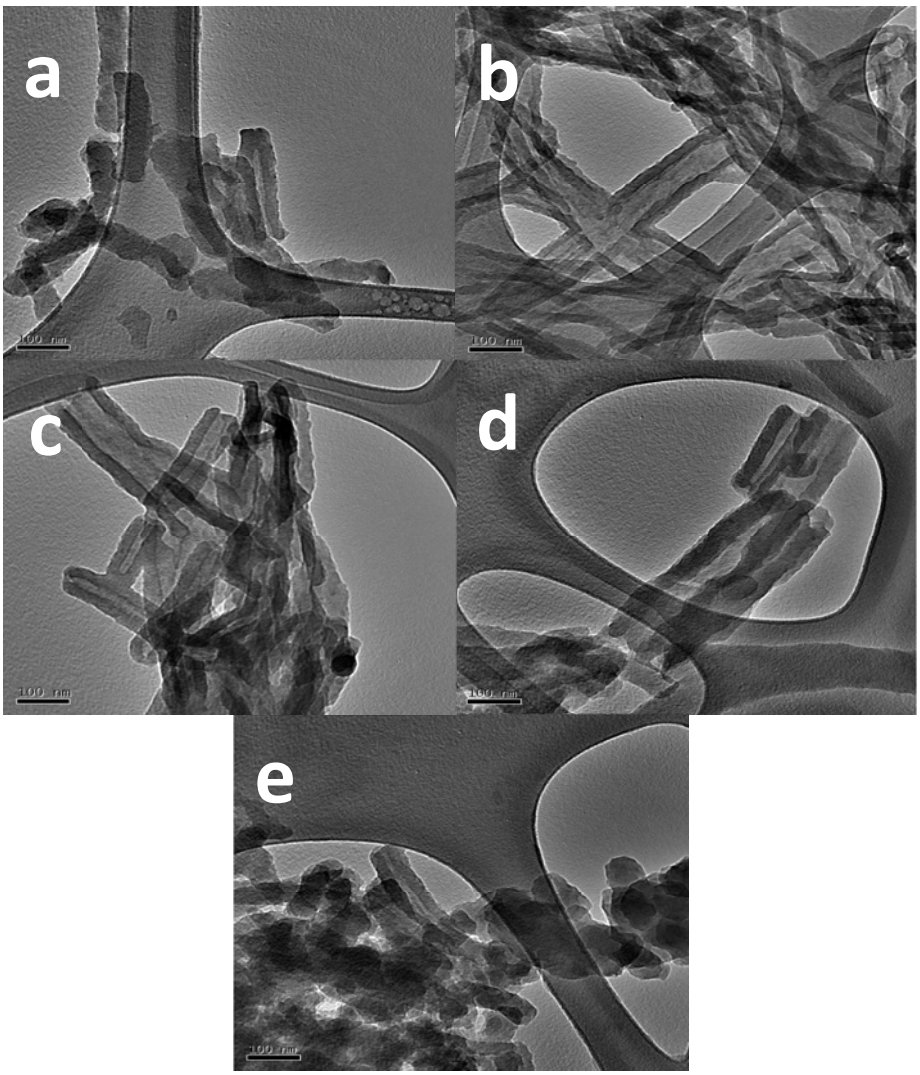

Fig. 5 TEM images of (a) $PANI^{0.5}$, (b) $PANI^{0.25}$, (c) $PANI^{0.1}$, (d) $PANI^{0.05}$ and (e) $PANI^{0.01}$.

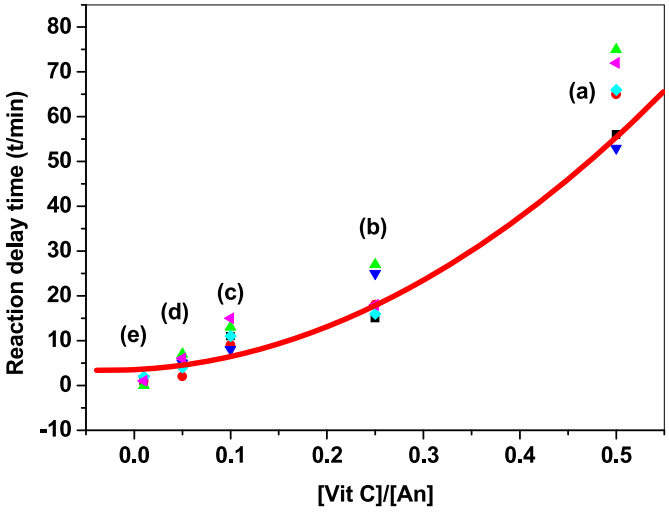

Fig. 6 Concentration of vitamin C vs. reaction delay time response for (a) $PANI^{0.5}$, (b) $PANI^{0.25}$, (c) $PANI^{0.1}$, (d) $PANI^{0.05}$ and (e) $PANI^{0.01}$.

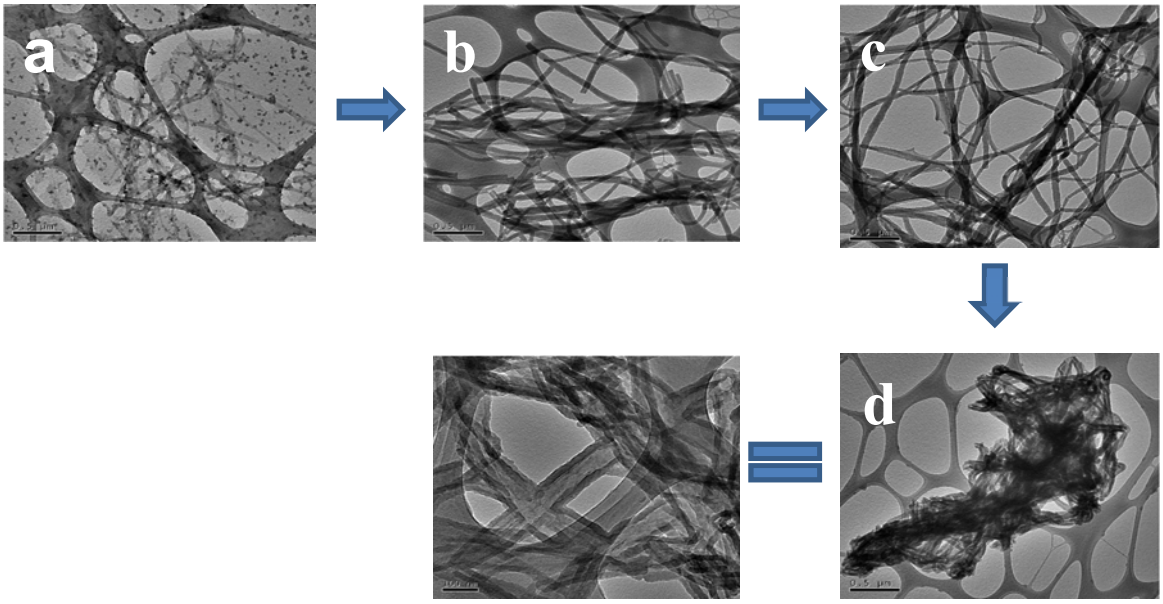

Fig. 7 FESEM images of the intermediate products after addition of initiator (a) 10 minutes, (b) 1 hour, (c) 4 hours and (d) final step after washing.

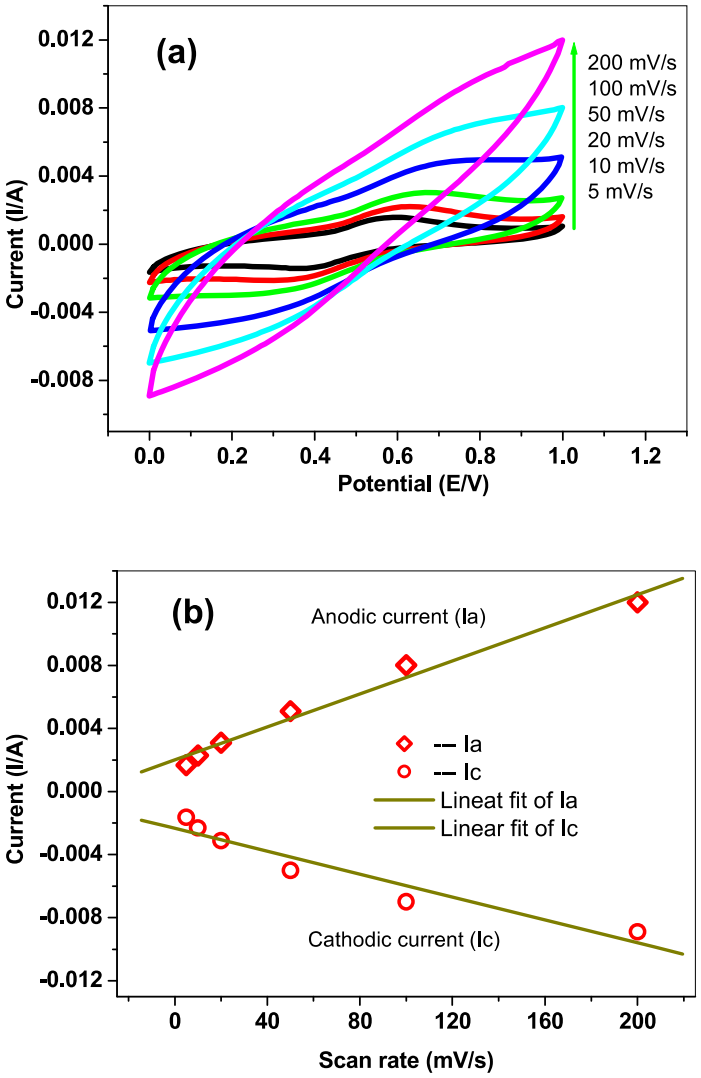

Fig. 8 Cyclic voltammogram of a) $PANI^{0.25,}$ in an aqueous 1 M H_2SO_4 electrolyte; (b) Plots of the peak current (the anodic peak current, Ia; the cathodic peak current, Ic) *vs* the scan rate.

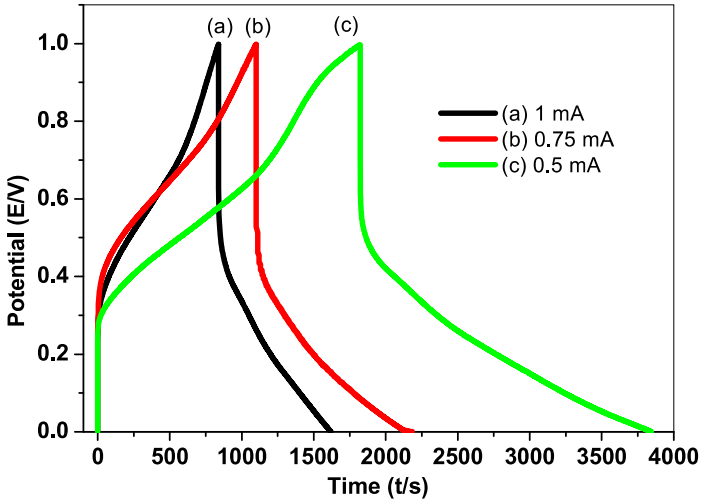

Fig. 9 Cyclic charge-discharge graph of $PANI^{0.25}$ at various scan rate in an aqueous 1 M H_2SO_4 electrolyte.

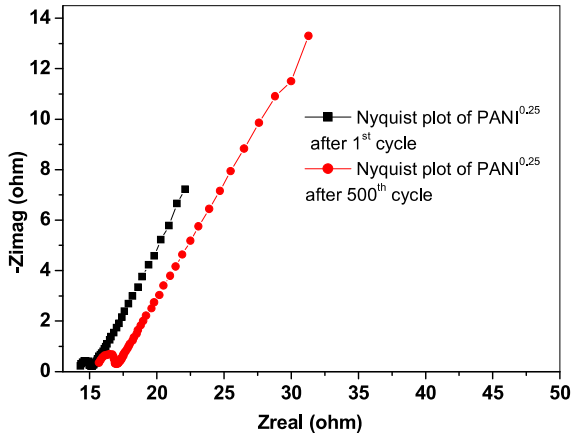

Fig.10 Impedance spectroscopy study of $PANI^{0.25}$ at various scan rate in an aqueous 1 M H_2SO_4 electrolyte.

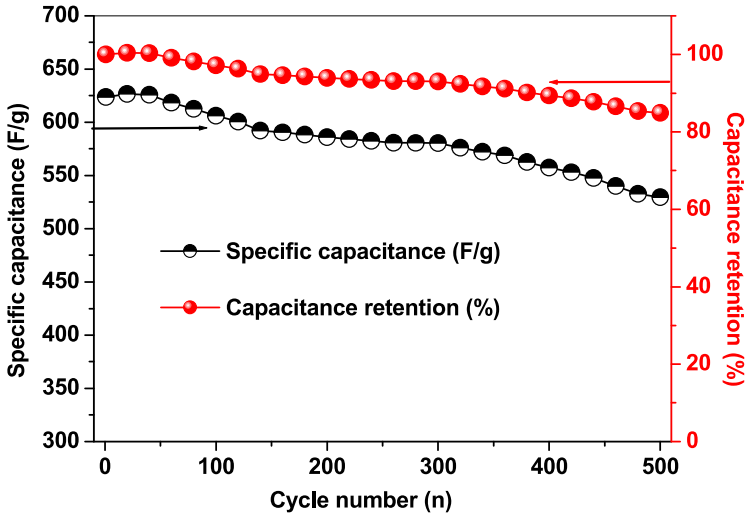

Fig. 11 Cyclic stability study of $PANI^{0.25}$ at various scan rate in an aqueous 1 M H_2SO_4 electrolyte.

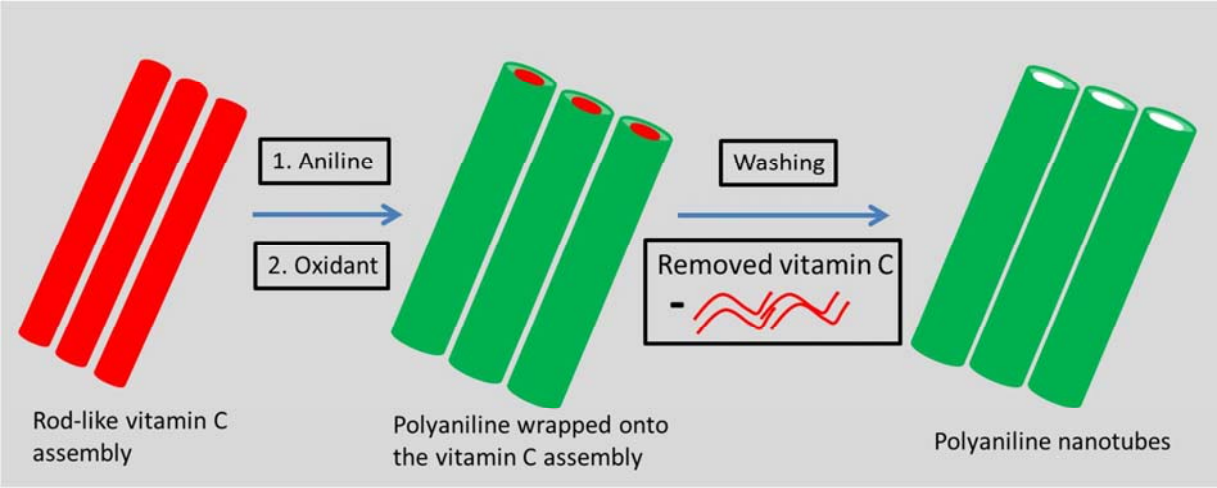

Scheme 1 Schematic diagram for the formation of polyaniline nanotubes.

Table 1 α values at different discharge currents

Discharge current density (mA)	Max. observed capacitance value (F/g)	α
1	619.76	0.5739
0.75	643.18	0.5966
0.5	714.68	0.6635

Figure captions:

Fig. 1 FTIR spectra of (a) pure vitamin C, (b) PANI/vitamin C at the molar ratio of 0.25 without washing and (c) pure PANI nanotube ($PANI^{0.25}$) at the molar ratio of 0.25 after washing. On right side is the enlarged spectrum of pure vitamin C.

Fig. 2 XPS spectra of N 1s of $PANI^{0.25}$ (narrow scan).

Fig. 3 XPS spectra of $PANI^{0.25}$ dispersed in water solvent.

Fig. 4 FESEM images of (a) $PANI^{0.5}$, (b) $PANI^{0.25}$, (c) $PANI^{0.1}$, (d) $PANI^{0.05}$ and (e) $PANI^{0.01}$.

Fig. 5 TEM images of (a) $PANI^{0.5}$, (b) $PANI^{0.25}$, (c) $PANI^{0.1}$, (d) $PANI^{0.05}$ and (e) $PANI^{0.01}$.

Fig. 6 Concentration of vitamin C vs. reaction delay time response for (a) $PANI^{0.5}$, (b) $PANI^{0.25}$, (c) $PANI^{0.1}$, (d) $PANI^{0.05}$ and (e) $PANI^{0.01}$.

Fig. 7 FESEM images of the intermediate products after addition of initiator (a) 10 minutes, (b) 1 hour, (c) 4 hours and (d) final step after washing.

Fig. 8 Cyclic voltammogram of a) $PANI^{0.25,}$ in an aqueous 1 M H_2SO_4 electrolyte; (b) Plots of the peak current (the anodic peak current, Ia; the cathodic peak current, Ic) *vs* the scan rate.

Fig. 9 Cyclic charge-discharge graph of $PANI^{0.25}$ at various scan rate in an aqueous 1 M H_2SO_4 electrolyte.

Fig. 10 Impedance spectroscopy study of $PANI^{0.25}$ at various scan rate in an aqueous 1 M H_2SO_4 electrolyte.

Fig. 11 Cyclic stability study of $PANI^{0.25}$ at various scan rate in an aqueous 1 M H_2SO_4 electrolyte.

Scheme caption:

Scheme 1 Schematic diagram for the formation of polyaniline nanotubes.

Table caption:

Table 1 α values at different discharge currents